2301-9069 (e)
1829-8370 (p)

KAPAL

Jurnal Ilmu Pengetahuan dan Teknologi Kelautan

journal homepage : http://ejournal.undip.ac.id/index.php/kapal

Vertical Motion Optimization of Series 60 Hull Forms Using Response Surface Methods

Budi Utomo[1)*)], Muhammad Iqbal[2)]

[1)] Department of Industrial Technology, Vocational School, Diponegoro University, Semarang 50275, Indonesia
[1)] Department of Naval Architecture, Faculty of Engineering, Diponegoro University, Semarang 50275, Indonesia
[*)] Corresponding Author : budiutomo_undip@yahoo.com

Article Info

Keywords:
Ship Vertical Motion,
Response Surface Method,
Series 60

Article history:
Received: 30/09/20
Last revised: 29/10/20
Accepted: 29/10/20
Available online: 31/10/20

DOI:
https://doi.org/10.14710/kapal.v17i3.33212

Abstract

There are many aspects to analyze seakeeping performance, one of which is the ship's vertical motion. As well-known, vertical motion and its derivatives, vertical velocity and acceleration, will be related to other aspects of seakeeping performance, such as slamming, deck wetness, and MSI. This study discusses optimizing the hull shape with small vertical motion using the Response Surface Methods (RSM). This research aims to minimize the ship's vertical motion so that the ship's performance is better than the initial one. Besides, this research was conducted to apply the RSM in the naval architecture field. The hull's shape used in this study is Series 60 hull form with a length of 31 m. The variables used for the optimization process are the ratio of L/B (X1) and B/T (X2) in the range of ± 10% with fixed displacement. Seakeeping analysis was carried out at a speed of 6.78 knots (Fr 0.2), a heading angle of 180°, and a significant wave height of 0.77 meters. The results show that the optimum model is found in Model 9 where the value of X1 = -2.94 or L/B = 6.71 and X2 = 5 or B/T = 2.75. Model 9 can reduce the vertical motion of the ship by 16.38%.

1. Introduction

The prediction of ship motion has become one of the most popular topics studied by naval architects. The ship cruising in waves will increase the resistance, which leads to an increase in fuel consumption. Several researchers conducted this analysis for economic purposes (to reduce additional ship resistance). An added resistance study was carried out on the container ship (KRISO)[1], catamaran [2], and trimaran [3]. Some of them use the Artificial Neural Network (ANN) method [4], 2.5 D Method [5], and Rankine-Panel Method [6]. Some researchers also discuss the uncertainty in calculating the added resistance in short regular waves [7].

Other researchers conducted a seakeeping analysis to consider the comfort and safety of passengers on board. Among them is the Motion Sickness Incident (MSI) analysis, a study that discusses the percentage of passengers who will get seasick when boarding a ship. MSI arises due to the ship's vertical movement caused by a combination of ship heaving and pitching. Several studies were carried out for passenger ships [8], catamaran [9], and fast vessels [10].

Apart from MSI, the vertical motion of ships also causes slamming and deck wetness phenomena. Slamming is the phenomenon of lifting the ship's bow from the surface of the sea level. Meanwhile, Deck Wetness (green water) occurs when the ship's deck enters the water's surface. These phenomena will make passengers uncomfortable if this phenomenon occurs continuously throughout the voyage with high intensity.

Research on slamming for trimaran ships with different conditions has been carried out by [11]. Some researchers use the SPH (Smoothed Particle Hydrodynamics) method [12]. Some researchers study slamming for the ship's bow structure using the Finite Element Method (FEM) [13]. Furthermore, the research for deck wetness was carried out by [14] and [15].

Due to the many aspects studied on seakeeping performance, some researchers use optimization tools to get the best hull shape. Among them are using Nondominated Sorting Genetic Algorithm II (NSGA II) to optimize trimaran ship outriggers to minimize heaving, pitching, and rolling motions [16]. Some researchers use the Genetic Algorithm (GA) to optimize the Passive Anti-Roll Tank to minimize the ship's rolling motion [17] and to minimize vertical motion of the Wigley and S60 hull forms [18]. The Multi-Objective Genetic Algorithm (MOGA) method is also used to obtain the best hull shape of fishing vessels by minimizing the vessel's seakeeping response [19]. Besides, there are also hull parametric studies to get the best shape of the ship, which has the best seakeeping performance [20].

As described above, many studies have been conducted on optimizing the hull shape related to seakeeping using Genetic Algorithm (GA). However, in this study, the authors used the Response Surface Method (RSM) as an optimization method. RSM is a convenient and economical optimization technique widely used to evaluate an experiment's variables that result in one or more responses [21].

Design Of Experiments (DoE) based on RSM does not require much trial/testing [22]. The results of the DoE are then made a mathematical model in the linear and quadratic form to get the maximum/minimum results. Several researchers have used this method to optimize several research variables. Among them are in the field of structure [23], [24], in the mechanical engineering field [25], [26], and very rarely used in the field of naval architecture as was done by [27] [28].

This research aims to minimize vertical motion so that the ship's performance is better than the initial one and also to apply RSM in the naval architecture field as a hull shape optimization tool. Passenger comfort can be increased by minimizing the ship's response to waves, such as movement, velocity, and acceleration response. Therefore, this optimization's objective function is to minimize the ship's vertical motion by varying the two main size ratio variables of the ship, namely X1 (L/B) and X2 (B/T).

2. Methods

The object of this research is the Series 60 (S60) ship. This ship hull form has been widely studied by other researchers at various scales, including research on seakeeping [29], [18], ship propulsion [30], catamaran resistance [31], Optimization of ship hydrodynamic performance in shallow waters [32]. The main dimension is shown in Table 1, while the 3D model of this ship is shown in Figure 1.

Table 1. Main Dimenison of Ship

Dimension	Value (m)
Lwl	30.976 m
B	4.343 m
T	1.737 m
Wetted Area	184.358 m^2
Displacement	163.9 ton
Volume (displaced)	159.911 m^3
CB	0.684
L/B	7.13
B/T	2.50

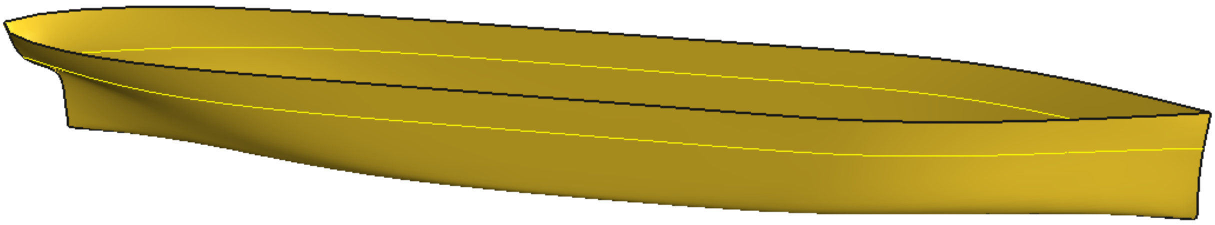

Figure 1. 3D Model of S60 Hull Form

The research begins with analyzing the ship motion response to regular waves described in the RAO (Response Amplitude Operator). The method for calculating the RAO value in this study uses Strip Theory at Fr 0.2 and a heading angle of 180°. For translational motion, RAO is a direct comparison between the amplitude of the ship's motion and the wave amplitude, both in length units (Equation 1). Meanwhile, RAO for rotational motion is the ratio between the amplitude of the ship's rotation motion (in radians) to the wave's slope (Equation 2).

$$RAO = \frac{Z_a\ (m)}{\zeta_a\ (m)} \tag{1}$$

$$RAO = \frac{\theta_a\ (rad)}{k\zeta_a\ (rad)} \tag{2}$$

The combination of heaving and pitching motion is used to determine vertical ship motion response at point FP. This response is expressed in RAO vertical motion at point FP (RAO_{vm}), which is the ratio between vertical motion with wave height at point CG. This Vertical Motion is called Absolute Vertical Motion, as shown in Equation 3.

$$RAO_{vm} = \frac{(Z_{FP})_a\ (m)}{\zeta\ (m)} \tag{3}$$

Equation 4 is used to find the vertical motion at the point FP. Z is the response of the ship's heaving motion (m), ξ is the distance between CG to the point FP (m), θ is the response of the ship's pitching motion (rad). Illustration of vertical motion at point FP is shown in Figure 2.

$$Z_{FP} = Z + \xi \, Sin\, \theta$$ (4)
$$Z_{FP} = Z_a \, Cos\,(\omega_e t + \varepsilon_z) + \xi \, \theta_a \, Cos\,(\omega_e t + \varepsilon_\theta)$$

$$Z_{FP} = (Z_{FP})_a \, Cos\,(\omega_e t + \varepsilon_b)$$
$$(Z_{FP})_a = \sqrt{{Z_a}^2 + (\xi\theta_a)^2 + 2\, Z_a \, \xi\theta_a Cos(\varepsilon_\theta)}$$
$$Tan\,(\varepsilon_b) = \frac{(Z_a)Sin(\varepsilon_z) + \xi\theta_a Sin(\varepsilon_\theta)}{(Z_a)Cos(\varepsilon_z) + \xi\theta_a Cos(\varepsilon_\theta)}$$

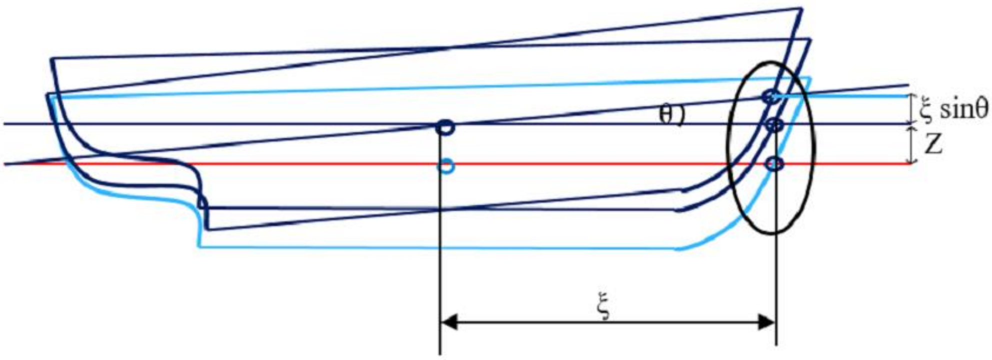

Figure 2. Illustration of Absolute Vertical Motion in FP

Furthermore, to describe the ship's response in random waves, it is necessary to analyze the response spectrum of ship motion, stated in Equation 5. This study's wave spectrum is Bretschneider with one parameter: the significant wave height parameter (Hs) (Equation 6). The significant wave height (Hs) used was 0.77 m. The RMS value of the ship's vertical motion (RMS VM) is expressed in Equation 7 with the value n = 0.

$$S_r(\omega) = (RAO_{vm})^2 \times S_w(\omega)$$ (5)

$$S_w(\omega) = \frac{A}{\omega^5} \exp\left(\frac{-B}{\omega^4}\right)$$ (6)

$$A = 0.00811\, g^2$$
$$B = \frac{3.11}{{H_s}^2}$$

$$RMS = \sqrt{m_n}$$ (7)
$$m_n = \int_0^\infty \omega^n S_r(\omega) d\omega$$

The RSM optimization process is carried out in 3 stages: 1) Order I, 2) Steepest Descent, and 3) Order II. Experimental design for first and third stage using CCD (Central Composite Design) with two factors/variables, namely L/B (X1) and B/T (X2). The minimum and maximum limits of the two variables are determined before the stage is carried out. This first stage produces a linear equation as in Equation 8.

$$Response\ Y = b_0 + b_1 X1 + b_2 X1$$ (8)

Next, the second stage is of Steepest Descent (or Ascent). This stage provides movement in a specific direction, which can be increased to a minimum or maximum value. Researchers utilize information from mathematical models (Equation 8) to describe specific responses instead of relying on intuition or guessing what experimental conditions should be done next. The response surface method (RSM) combined with the Steepest Descent approach is an excellent technique for optimizing response. This has been successfully demonstrated by [33].

Based on Equation 8, the trend of response results will be linear. However, if the trend of the experimental results proves that there is a turning point (the trend will be non-linear), then the next step is Stage 3 (Order II), as done by [27] and [28]. The turning point of X1 and X2 results from Steepest Descent became the initial models in Stage 3. Same with Stage 1, the minimum and maximum limits of X1 and X2 of Stage 3 are predetermined.

In this research, the target achieved is to find X1 and X2, which produce a minimum vertical ship motion point. The limits of X1 and X2 for all stages are determined not to exceed ± 10% of the initial conditions to obtain a feasible hull shape. The conditions for changing the L/B and B/T variables were carried out with fixed displacement. This condition is done to make the response of the ship's vertical motion unaffected by ship displacement.

3. Results and Discussion

3.1. Order I

The Design of Experiment based on the Center Composite Design in stage 1 is shown in Table 3. At this stage, the maximum and minimum values of the two variables are determined to be ± 2% so that if there is a development of variable towards the optimum point, it does not exceed ± 10%, as shown in Table 2. The initial variable value is coded 0, the maximum value is coded 1, while the minimum value is coded -1.

Table 2. Codification of Maximum and Minimum Values in Order I

Code	**-1**	**0**	**1**
X1 (L/B)	6.99	7.13	7.28
X2 (B/T)	2.45	2.50	2.55

Each experiment resulted in 1 different ship model. Furthermore, each model has analyzed its motion response according to the conditions mentioned in the methods chapter. The vertical motion response results from the five models (Table 3) are regressed to produce a linear function containing the variables X1 and X2, as shown in Equation 9. This equation has a value of R^2 = 0.997, where this value can be considered valid enough to be used.

Table 3. Design of Experiment Orde I and Its Responses (RMS Vertical Motion)

Model	**Code**		**Parameters**		**RMS Vertical Motion (m)**
	X1	X2	L/B	B/T	
Initial	0	0	7.13	2.50	0.354
1	1	1	7.28	2.55	0.350
2	1	-1	7.28	2.45	0.368
3	-1	1	6.99	2.55	0.341
4	-1	-1	6.99	2.45	0.357

$$RMS\ VM = 0.354 + 0.005(X1) - 0.0085(X2) \tag{9}$$

3.2. Steepest Descent

This process serves to determine the turning point of the vertical motion, which continues to fall and is no longer following the prediction from Equation 9. The turning point is an indication that the response trend is non-linear. If a turning point is found, the second-order stage can be continued where at this stage, the resulting regression is a quadratic function. The minimum point position can easily be determined by satisfying the condition where the first derivative of the function VM for X1 and X2 is zero, respectively.

Based on each factor's coefficient in the Order I model (Equation 9), the difference in coefficient change (ΔXn) is calculated to carry out the steepest descent process. The largest regression coefficient in Equation 9 is chosen as the basis value. As mentioned in [33] and [34], the coefficient value used as the basis is chosen based on the highest value.

Based on Equation 9, the largest coefficient is in X2, which is 0.0085. Using the X2 coefficient as the basis, Equations 10 and 11 are obtained. Furthermore, the steepest descent process and the vertical motion response results are shown in Table 4 and Figure 3.

$$\Delta X1 = \frac{0.005}{-0.0085} = -0.5882 \tag{10}$$

$$\Delta X2 = \frac{-0.0085}{-0.0085} = 1 \tag{11}$$

Table 4. Steepest Descent and Its Responses (RMS Vertical Motion)

Model	**Code**		**Parameters**		**RMS Vertical Motion (m)**
	X1	X2	L/B	B/T	
Initial	0	0	7.13	2.50	0.354
5	-0.5882	1	7.05	2.55	0.343
6	-1.1764	2	6.96	2.60	0.331
7	-1.7646	3	6.88	2.65	0.318
8	-2.3528	4	6.80	2.70	0.307
9	-2.9410	5	6.71	2.75	0.296

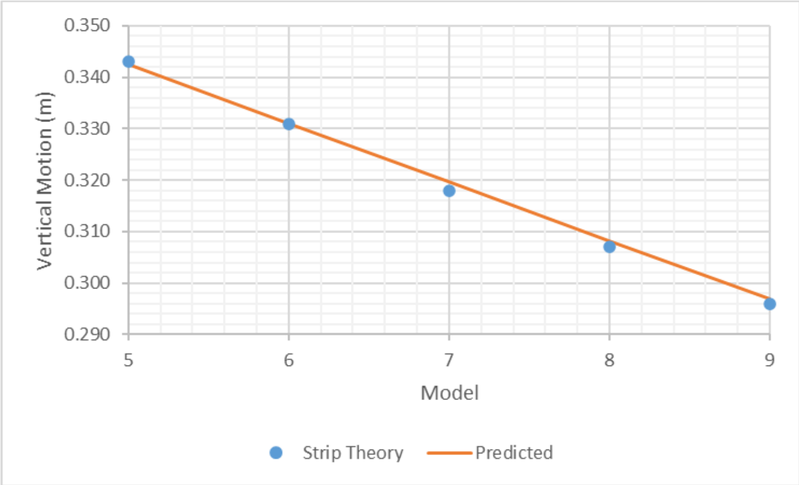

Figure 3. Steepest Descent Results

Table 4 illustrates that each change in X2 is 1 (∆X2 = 1), then the change in X1 is -0.5882 (∆X1 = -0.5882). Experiments were carried out until Model 9, where the B/T value had reached the maximum limit of 10%, namely 2.75. However, there is no turning point in this condition, which indicates that the tendency of the ship's vertical response, in this case, is linear. Therefore, the Second Order Phase did not need to be continued.

3.3. Optimum Model

Based on Table 4 and Figure 3, the optimal conditions are found in Model 9, where X1 = -2.941 or L/B = 6.71 and X2 = 5 or B/T = 2.75. Comparison of the Main Dimension of the Initial Model and Model 9 is presented in Table 5. The L/B value decreased by almost 6%, while the B/T value increased by 10%. The optimal model reduces the ship's length like L/B reduction in percentage and reduces the vessel draught by more than 9%. In order to get the same displacement, the CB value has increased by almost 17%. The visual comparison of the shape of the ship is shown in Figure 4.

Table 5. Comparison of the Main Dimension of the Ship

Dimension	Value		Difference
	Initial Model	Model 9 (Optimal)	(%)
Lwl (m)	30.976	29.154	-5.88
B (m)	4.343	4.343	0.00
T (m)	1.737	1.579	-9.10
Wetted Area (m^2)	184.358	182.427	-1.05
Displacement (ton)	163.9	163.8	-0.06
Volume (displaced) (m^3)	159.911	159.843	-0.04
CB (-)	0.684	0.80	16.96
L/B (-)	7.13	6.71	-5.89
B/T (-)	2.50	2.75	10.00

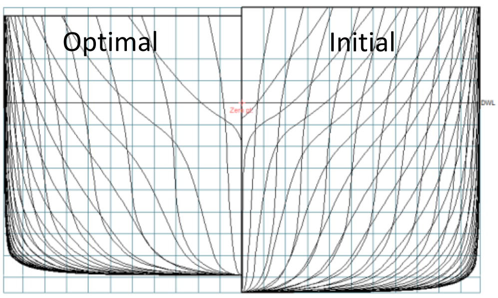

(a)

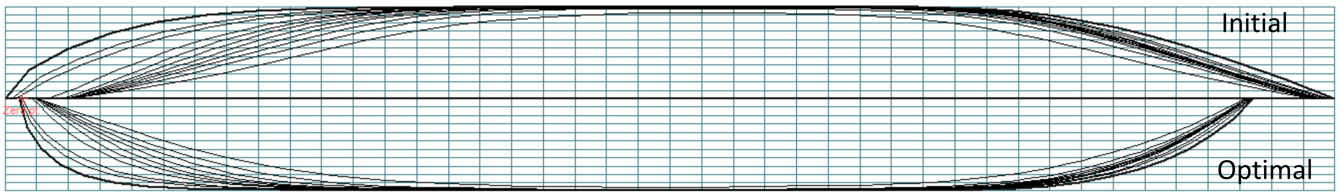

(b)

Figure 4.Comparison of the Hull Model Front View (a) and Top View (b)

This optimal model is in line with [18] that the optimal shape of S60 in reducing vertical motion with the Genetic Algorithm (GA) method reduces the length of the ship. Besides, the ship's vertical motion can also be reduced due to the increase in B/T and CB values, according to [35]. Comparing the RAO motion of Heaving, Pitching, and RAO of Vertical Motion is shown in Figure 5, Figure 6, and Figure 7.

Following Equation 4, the value of vertical motion is the sum of the heaving and pitching motions. If these two values are small, then the value for vertical motion will also be small. Figure 5 shows the RAO curve of the ship heaving motion. It can be seen that the peak RAO heaving of Model 9 is reduced by 29.36% from the initial 1.61 at 1.88 rad/s to 1.14 at 1.91 rad/s. Figure 6 shows the RAO Pitching comparison, where the optimal model RAO peak is reduced by 14.57% from 1.23 at 1.67 rad/s to 1.05 at 1.40 rad/s. As shown in both figures, Model 9 reduces both the RAO peak of Heaving and Pithing motion, minimizing the ship's vertical motion, as shown in Figure 7.

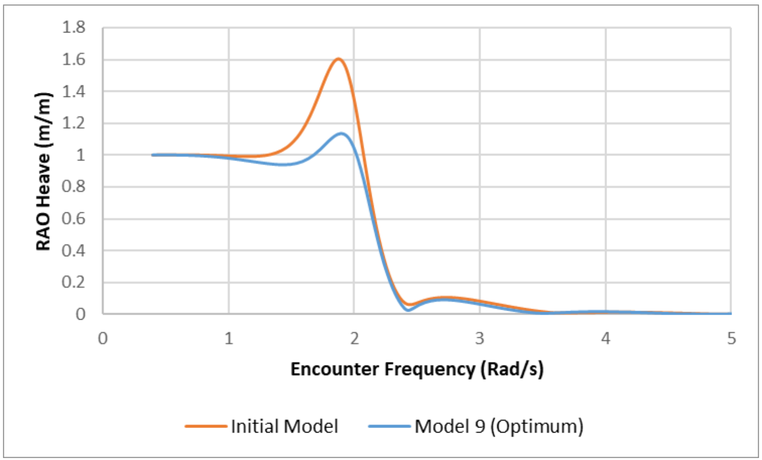

Figure 5. Heaving RAO

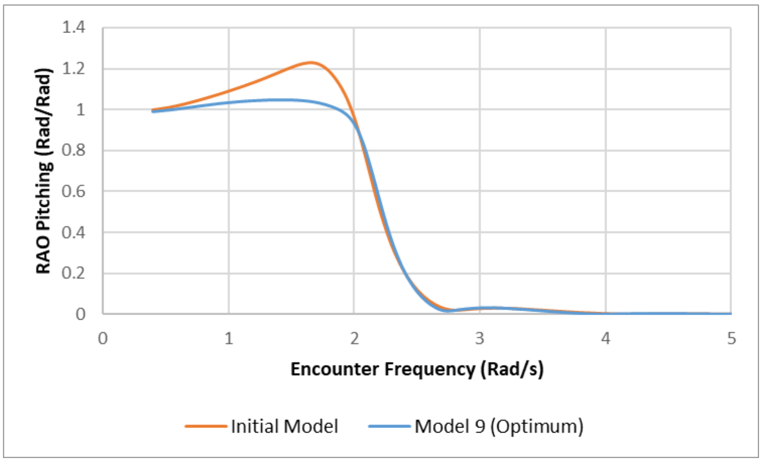

Figure 6. Pitching RAO

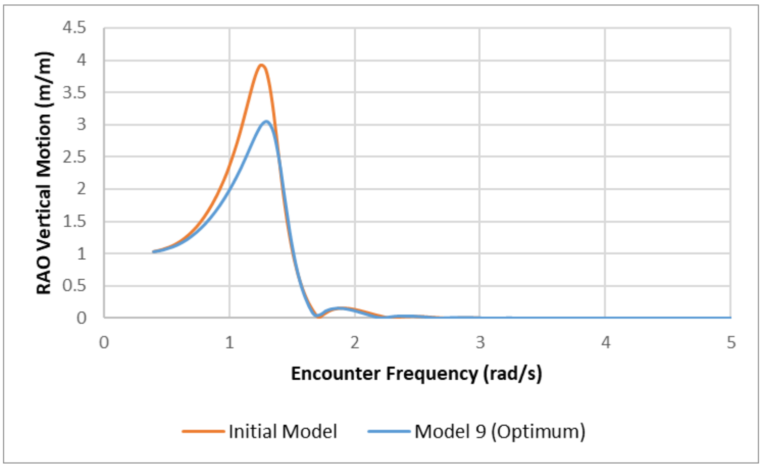

Figure 7. RAO of Vertical Motion at FP

Figure 7 depicts the RAO of vertical motion in FP. RAO peak of Model 9 decreased by 22.60% from 3.93 at 1.25 rad/s to 3.04 at 1.31 rad/s. However, by using GA optimization, the RAO peak of S60 Vertical Hull Motion was reduced by 27% [18]. This difference is due to the different optimization methods used. Also, the point used in [18] is 0.15 LPP behind FP (not precisely at the FP point as in this study). So that, the distance between the point of observation and CG (ξ), as shown in Equation 4, is also reduced.

However, this research proves that apart from the Genetic Algorithm method, RSM optimization can be used well in optimizing the ship's main dimension, in this case, the ratio of L/B and B/T, to produce a minimum vertical motion of the ship.

4. Conclusion

Based on this research, the optimum model is found in Model 9 where the value of X1 = -2.94 or L/B = 6.71 and X2 = 5 or B/T = 2.75. Model 9 can reduce the vertical motion of the ship by up to 16.38%. This research proves that the RSM optimization can be used properly and is quite powerful in optimizing the ship's main dimension to produce minimum vertical motion.

References

[1] E. Shivachev, M. Khorasanchi, S. Day, and O. Turan, "Impact of trim on added resistance of KRISO container ship (KCS) in head waves: An experimental and numerical study," *Ocean Engineering*, vol. 211, p. 107594, 2020.

[2] W. He, M. Diez, Z. Zou, E. F. Campana, and F. Stern, "URANS study of Delft catamaran total/added resistance, motions and slamming loads in head sea including irregular wave and uncertainty quantification for variable regular wave and geometry," *Ocean Engineering*, vol. 74, pp. 189–217, 2013.

[3] J. Gong, S. Yan, Q. Ma, and Y. Li, "Added resistance and seakeeping performance of trimarans in oblique waves," *Ocean Engineering*, vol. 216, p. 107721, 2020.

[4] T. Cepowski, "The prediction of ship added resistance at the preliminary design stage by the use of an artificial neural network," *Ocean Engineering*, vol. 195, p. 106657, 2020.

[5] W. Y. Duan, S. M. Wang, and S. Ma, "Verification of application of the 2.5 D method in high-speed trimaran vertical motion and added resistance prediction," *Ocean Engineering*, vol. 187, p. 106177, 2019.

[6] W. Zhang and O. el Moctar, "Numerical prediction of wave added resistance using a Rankine Panel method," *Ocean Engineering*, vol. 178, pp. 66–79, 2019.

[7] N. Sogihara, M. Tsujimoto, R. Fukasawa, and T. Hamada, "Uncertainty analysis for measurement of added resistance in short regular waves: Its application and evaluation," *Ocean Engineering*, vol. 216, p. 107823, 2020.

[8] A. Scamardella and V. Piscopo, "Passenger ship seakeeping optimization by the Overall Motion Sickness Incidence," *Ocean Engineering*, vol. 76, pp. 86–97, 2014.

[9] V. Piscopo and A. Scamardella, "The overall motion sickness incidence applied to catamarans," *International Journal of Naval Architecture and Ocean Engineering*, vol. 7, no. 4, pp. 655–669, 2015.

[10] E. López, F. J. Velaseo, T. M. Rueda, and E. Moyano, "Experiments on the Reduction of Motion Sickness Incidence on a High-Speed Craft," *IFAC Proceedings Volumes*, vol. 36, no. 21, pp. 97–102, 2003.

[11] Z. Sun, Y. Z. Deng, L. Zou, and Y. C. Jiang, "Investigation of trimaran slamming under different conditions," *Applied Ocean Research*, p. 102316, 2020.

[12] H. Cheng, F. R. Ming, P. N. Sun, Y. T. Sui, and A.-M. Zhang, "Ship hull slamming analysis with smoothed particle hydrodynamics method," *Applied Ocean Research*, vol. 101, p. 102268, 2020.

[13] B. Yang and D. Wang, "Numerical study on the dynamic response of the large containership' s bow structure under slamming pressures," *Marine Structures*, vol. 61, pp. 524–539, 2018.

[14] B. Shabani, J. Lavroff, D. S. Holloway, M. R. Davis, and G. A. Thomas, "The effect of centre bow and wet-deck geometry on wet-deck slamming loads and vertical bending moments of wave-piercing catamarans," *Ocean Engineering*, vol. 169, pp. 401–417, 2018.

[15] M. R. Davis and J. R. Whelan, "Computation of wet deck bow slam loads for catamaran arched cross sections," *Ocean Engineering*, vol. 34, no. 17–18, pp. 2265–2276, 2007.

[16] S. M. Wang, S. Ma, and W. Y. Duan, "Seakeeping optimization of trimaran outrigger layout based on NSGA-II," *Applied Ocean Research*, vol. 78, pp. 110–122, 2018.

[17] R. Subramanian, P. V Jyothish, and others, "Genetic Algorithm Based Design Optimization of a Passive Anti-Roll Tank in a Sea Going Vessel," *Ocean Engineering*, vol. 203, p. 107216, 2020.

[18] H. Bagheri, H. Ghassemi, and A. Dehghanian, "Optimizing the seakeeping performance of ship hull forms using genetic algorithm," *TransNav: International Journal on Marine Navigation and Safety of Sea Transportation*, vol. 8, no. 1, pp. 49–57, 2014.

[19] M. A. Gammon, "Optimization of fishing vessels using a Multi-Objective Genetic Algorithm," *Ocean Engineering*, vol. 38, no. 10, pp. 1054–1064, 2011.

[20] S. Özüm, B. Sener, and H. Yilmaz, "A parametric study on seakeeping assessment of fast ships in conceptual design stage," *Ocean Engineering*, vol. 38, no. 13, pp. 1439–1447, 2011.

[21] M. A. Bezerra, R. E. Santelli, E. P. Oliveira, L. S. Villar, and L. A. Escaleira, "Response surface methodology (RSM) as a tool for optimization in analytical chemistry," *Talanta*, vol. 76, no. 5, pp. 965–977, 2008.

[22] L. Ma, Y. Han, K. Sun, J. Lu, and J. Ding, "Optimization of acidified oil esterification catalyzed by sulfonated cation exchange resin using response surface methodology," *Energy Conversion and Management*, vol. 98, pp. 46–53, 2015.

[23] A. Baroutaji, M. D. Gilchrist, D. Smyth, and A.-G. Olabi, "Crush analysis and multi-objective optimization design for circular tube under quasi-static lateral loading," *Thin-Walled Structures*, vol. 86, pp. 121–131, 2015.

[24] X. Wang *et al.*, "Combining the finite element method and response surface methodology for optimization of shot peening parameters," *International Journal of Fatigue*, vol. 129, p. 105231, 2019.

[25] O. I. Awad *et al.*, "Response surface methodology (RSM) based multi-objective optimization of fusel oil-gasoline blends at different water content in SI engine," *Energy Conversion and Management*, vol. 150, pp. 222–241, 2017.

[26] M. Anwar, M. G. Rasul, and N. Ashwath, "Production optimization and quality assessment of papaya (Carica papaya) biodiesel with response surface methodology," *Energy Conversion and Management*, vol. 156, pp. 103–112, 2018.

[27] M. Iqbal, E. S. Hadi, and G. Pranamya, "Geometry Optimization Of Centre Bulb To Reduce Wave Resistance On Catamaran Ship," in *International Conference on Ship and Offshore Technology (ICSOT) Indonesia*, 2019.

[28] R. Kuasa, E. S. Hadi, and M. Iqbal, "Optimalisasi Curve Linesplan Haluan Kapal Perintis 750 DWT Menggunakan Response Surface Methode (RSM) untuk Mengurangi Hambatan," *Jurnal Teknik Perkapalan*, vol. 5, no. 4, 2017.

[29] M. S. Baree and L. Afroz, "Seakeeping Performance of Series 60 Ships," *Procedia engineering*, vol. 194, pp. 189–196, 2017.

[30] H. Nowruzi and A. Najafi, "An experimental and CFD study on the effects of different pre-swirl ducts on propulsion performance of series 60 ship," *Ocean Engineering*, vol. 173, pp. 491–509, 2019.

[31] A. Souto-Iglesias, D. Fernández-Gutiérrez, and L. Pérez-Rojas, "Experimental assessment of interference resistance for a Series 60 catamaran in free and fixed trim-sinkage conditions," *Ocean Engineering*, vol. 53, pp. 38–47, 2012.

[32] G. K. Saha, K. Suzuki, and H. Kai, "Hydrodynamic optimization of ship hull forms in shallow water," *Journal of Marine Science and Technology*, vol. 9, no. 2, pp. 51–62, 2004.

[33] A. P. Joyce and S. S. Leung, "Use of response surface methods and path of steepest ascent to optimize ligand-binding assay sensitivity," *Journal of Immunological Methods*, vol. 392, no. 1–2, pp. 12–23, 2013.

[34] M. R. Hasniyati, H. Zuhailawati, R. Sivakumar, and B. K. Dhindaw, "Optimization of multiple responses using overlaid contour plot and steepest methods analysis on hydroxyapatite coated magnesium via cold spray deposition," *Surface and Coatings Technology*, vol. 280, pp. 250–255, 2015.

[35] A. Kükner and K. Sariöz, "High speed hull form optimisation for seakeeping," *Advances in Engineering Software*, vol. 22, no. 3, pp. 179–189, 1995.